Aerosol-Assisted Chemical Vapor Deposition of NbS_2 and TaS_2 Thin Films from Pentakis(dimethylamido)metal Complexes and 2-Methylpropanethiol

Emily S. Peters,[a] Claire J. Carmalt,*[a] Ivan P. Parkin,[a] and Derek A. Tocher[a]

Keywords: Niobium disulfide / Tantalum sulfide / Thin film / Aerosol-assisted CVD

Thin films of NbS_2 and TaS_2 have been produced from $[M(NMe_2)_5]$ (M = Nb, Ta) and *t*BuSH by aerosol-assisted chemical vapor deposition on glass. Gold-colored, reflective films were obtained and deposition took place at 250–350 °C for NbS_2 and 225–450 °C for TaS_2 using dichloromethane or hexanes as solvent. The niobium and tantalum sulfide films were analyzed by Raman spectroscopy, scanning electron microscopy (SEM), X-ray powder diffraction, energy dispersive analysis of X-rays (EDAX) and X-ray photoelectron spectroscopy (XPS). In order to identify possible compounds present in the aerosol mist, the solution phase reaction of $[M(NMe_2)_5]$ and five equivalents of *t*BuSH in toluene at room temperature was carried out. Yellow crystals of the partially substituted tantalum thiolate $[Ta(S\text{-}tBu)_2(NMe_2)_3]$ were isolated. The X-ray structure of $[Ta(S\text{-}tBu)_2(NMe_2)_3]$ has been determined.

The layered transition-metal dichalcogenides, which include tantalum disulfide and niobium disulfide, exhibit a number of interesting properties as a result of their structure. Thus, the layered structure has resulted in transition-metal dichalcogenides having diverse applications, such as high-temperature lubricants, catalysts and also in photovoltaic cells.[1–3] Tantalum disulfide in particular has been tested for use in lithium ion batteries, while NbS_2 has been shown to be an effective humidity sensor, in addition to uses as a catalyst in hydrotreating petroleum cuts.[4–9] These applications require a high surface area for optimum performance suggesting that thin film formation would be favorable. However, there are only limited reports of thin film formation of either NbS_2 or TaS_2.[3,10–15]

Physical deposition of NbS_2 films has been achieved by dipping the substrate into a NbS_2 powder layer, lying at the interface between water and an organic solvent.[5,10] This produced films with the basal planes parallel to the substrate's surface. Chemical vapor deposition (CVD) from single-source precursors of the form $[NbCl_4(S_2R_2)_2][NbCl_6]$ [R = CH_3 or $CH(CH_3)_2$] produced mixed NbS_2/Nb_2O_5 films.[11] However, the films formed were very thin (≤1000 Å) due to insufficient volatility of the precursors. Niobium monosulfide (NbS) films were deposited by low-pressure CVD from the homoleptic niobium thiolate $[Nb(SC_6H_3Me_2\text{-}2,6)_5]$.[12] We have recently reported the formation of NbS_2 films by atmospheric pressure CVD from the reaction of $NbCl_5$ with a range of sulfur precursors.[13] It was found that reaction of $NbCl_5$ with sulfides $[S(SiMe_3)_2$ or $tBu_2S_2]$ produced a new 1T-NbS_2 polytype. Conversely, reaction of $NbCl_5$ with thiols [*t*BuSH or $HS(CH_2)_2SH$] produced the known 3R-NbS_2 polytype. Reports of TaS_2 films have been limited to physical deposition routes.[14,15]

To the best of our knowledge, this paper represents the first thin film growth of TaS_2 by CVD and a novel aerosol-assisted (AA)CVD route to MS_2 (M = Nb, Ta) from $[M(NMe_2)_5]$ and *t*BuSH. Different and unique morphologies of films can be obtained by AACVD due to the influence of the solvent on the deposition, which could potentially lead to improved properties. Furthermore, thin films can be deposited under AACVD conditions at low temperatures and require only minimal amounts of precursor (ca. 0.1 g). In this study, niobium and tantalum thiolates were generated in situ from the reaction of $[M(NMe_2)_5]$ and *t*BuSH in hexanes or dichloromethane. An aerosol of this reaction mixture was then passed over a heated glass substrate, which resulted in the deposition of thin films of niobium and tantalum sulfide. The synthesis and crystal structure of the tantalum thiolate precursor $[Ta(S\text{-}tBu)_2(NMe_2)_3]$, prepared from the solution phase reaction of $[Ta(NMe_2)_5]$ and *t*BuSH, is also reported. Previous reports of the reaction of transition-metal amides with thiols suggest that complete substitution of the amide ligands is not achieved.[16,17] For example, the reaction of $[Ta(NMe_2)_5]$ with an excess of 2,6-dimethylthiophenol resulted in the substitution of four thiolate ligands forming $[Ta(SC_6H_3Me_2\text{-}2,6)_4(NMe_2)]$.[17]

Results and Discussion

Aerosol-Assisted Chemical Vapor Deposition

Gold-colored, reflective films have been deposited on glass from the dual-source AACVD reaction of

[a] Department of Chemistry, University College London, 20 Gordon Street, London, WC1H 0AJ, UK
E-mail: c.j.carmalt@ucl.ac.uk

 DOI: 10.1002/ejic.200500400

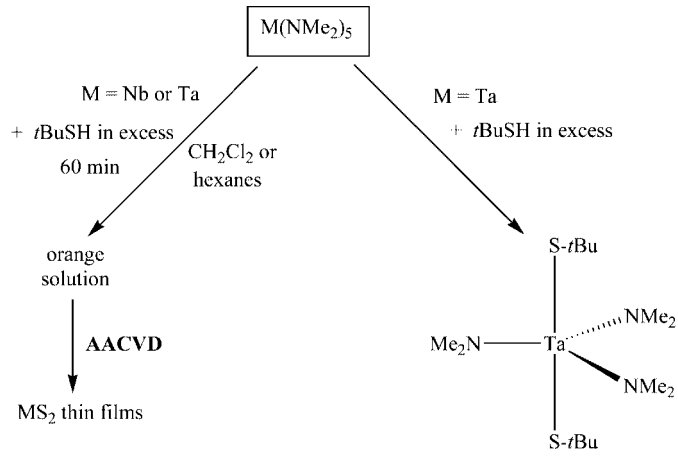

Scheme 1.

$[M(NMe_2)_5]$ (M = Nb, Ta) and *t*BuSH (Scheme 1). The reaction of $[M(NMe_2)_5]$ (M = Nb, Ta) and excess *t*BuSH in hexanes or dichloromethane was assumed to generate in situ the homoleptic metal thiolate, $[M(S\text{-}tBu)_5]$. However, solution phase studies (vida supra) indicate that this reaction could be incomplete and the bubbler would probably comprise of a mixture of $[M(S\text{-}tBu)_x(NMe_2)_{5-x}]$ (x = 0–5). Deposition was observed on both the top plate and the substrate due to larger particles formed by gas phase nucleation being unable to diffuse through the boundary layer at the substrate surface. However, the films deposited on the top plate correspond to those on the substrate but at a lower (50–75 °C) temperature (as measured). Niobium sulfide films were deposited between 250 and 350 °C and tantalum sulfide films were deposited between 225 and 450 °C (Table 1). The films deposited at the higher temperatures were localized towards the front of the substrate, which is an effect of fast film-growth kinetics. As the temperature was reduced complete substrate coverage was achieved. The gold color of the films is consistent with NbS_2 films grown by dual-source CVD routes at atmospheric pressure.[13] The films were adherent to the substrate, passing the Scotch Tape test. However, they were readily scratched by a brass or stainless steel stylus. The films remained unchanged after immersion in toluene, dichloromethane, THF, ether or acetonitrile for 1 month. The tantalum sulfide films were also unchanged by immersion in HCl for 1 month although the niobium sulfide films dissolved after one day. However, the niobium and tantalum sulfide films dissolved within minutes on immersion in HNO_3.

The reflectance and transmission spectra indicated that the gold-colored niobium sulfide films had good reflectance and minimal transmission (approx. 5%) in the region 400–1000 nm. The reflectance was fairly low in the visible region (approx. 15–20%) but increased to approx. 35% in the IR region. Four-point probe measurements suggest that the niobium sulfide films are metallic conductors at room temperature, as expected. Accurate readings could not be obtained as the films were scratched by the probe causing the reading to fluctuate. The tantalum sulfide films did not transmit at any wavelength and had a low reflectance (max. 15%).

Table 1. Deposition conditions and analysis of the films grown from the AACVD of $[M(NMe_2)_5]$ (M = Nb, Ta) and *t*BuSH.

Precursors	T [°C]	Solvent	EDXA
$Nb(NMe_2)_5$/*t*BuSH	350	dichloromethane	$NbS_{2.0}$
$Nb(NMe_2)_5$/*t*BuSH	300	dichloromethane	$NbS_{1.9}$
$Nb(NMe_2)_5$/*t*BuSH	250	dichloromethane	$NbS_{1.8}$
$Nb(NMe_2)_5$/*t*BuSH	300	hexanes	$NbS_{1.9}$
$Nb(NMe_2)_5$/*t*BuSH	250	hexanes	$NbS_{1.6}$
$Ta(NMe_2)_5$/*t*BuSH	450	dichloromethane	$TaS_{2.1}$
$Ta(NMe_2)_5$/*t*BuSH	350	dichloromethane	$TaS_{1.6}$
$Ta(NMe_2)_5$/*t*BuSH	450	hexanes	$TaS_{2.0}$
$Ta(NMe_2)_5$/*t*BuSH	400	hexanes	$TaS_{2.1}$
$Ta(NMe_2)_5$/*t*BuSH	350	hexanes	$TaS_{1.9}$
$Ta(NMe_2)_5$/*t*BuSH	300	hexanes	$TaS_{2.1}$
$Ta(NMe_2)_5$/*t*BuSH	250	hexanes	$TaS_{2.1}$
$Ta(NMe_2)_5$/*t*BuSH	225	hexanes	$TaS_{2.0}$

The niobium and tantalum sulfide films were characterized using a range of techniques. EDAX analysis shows the films are homogeneous and have a metal to sulfur ratio close to 1:2 over a number of spots (Table 2). The deviations from the MS_2 stoichiometry occurred primarily for the films deposited at lower temperatures, which were thinner meaning that a significant amount of the underlying glass was incorporated in the quantification. XPS of the niobium peaks in the NbS_2 films show that there is a single niobium environment with binding energies of 207.9 and 210.7 eV for $3d_{5/2}$ and $3d_{3/2}$, respectively. This matches well with the previously reported $3d_{5/2}$ value of 207.7 eV for bulk NbS_2.[19] However, ca. 2 atom-% nitrogen contamination was found by XPS in the films suggesting that complete reaction of the niobium amide with thiol to afford the homoleptic niobium thiolate had not occurred. Carbon and oxygen were found on the surface of the films by XPS, but these were removed by sputtering to leave the bulk of the film consisting of niobium and sulfur. The XPS of the tantalum in the TaS_2 films gave peaks at 23.5 and 25.4 eV corresponding to Ta $4f_{7/2}$ and $4f_{5/2}$ (Figure 1), which match well with published values for TaS_2 ($4f_{7/2}$, 23.8 eV; $4f_{5/2}$,

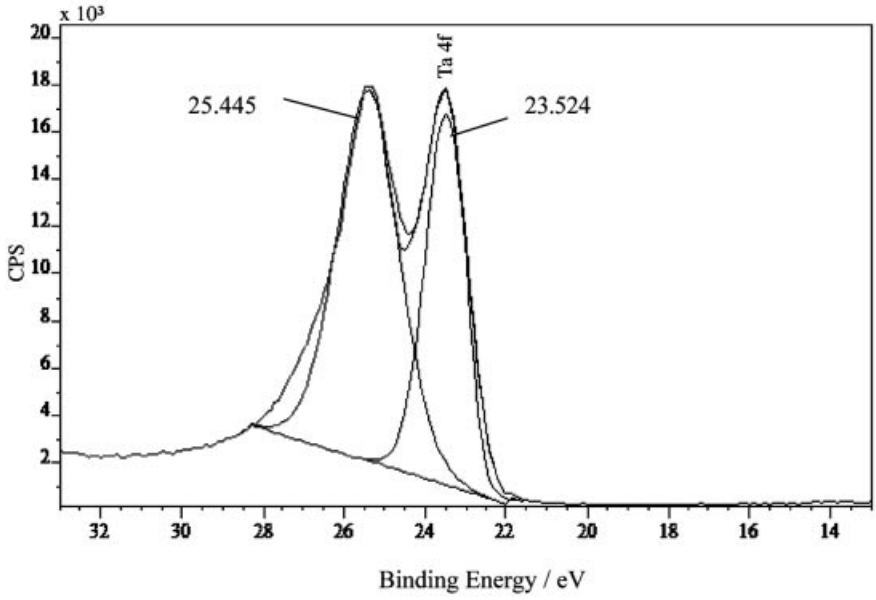

Figure 1. XPS of the Ta 4f peaks from a film deposited by AACVD from the in situ reaction of $[Ta(NMe_2)_5]$ and *t*BuSH at 450 °C.

25.7 eV).[20] Again, carbon and oxygen were found on the surface of the films by XPS but these were removed by sputtering to leave the bulk of the film comprised of tantalum and sulfur. The XPS of the TaS_2 films shows that there is also only one sulfur environment present with binding energies of 161.3 and 162.5 eV, corresponding to S $2p_{3/2}$ and $2p_{1/2}$, respectively.

All the films deposited were amorphous to X-rays even at the highest deposition temperatures. In comparison, NbS_2 films grown at 350–600 °C by atmospheric-pressure CVD from $NbCl_5$ and *t*BuSH were nanocrystalline; films deposited below 350 °C were amorphous.[13] The Raman pattern obtained for the NbS_2 films formed in this study (AACVD of $[Nb(NMe_2)_5]$/*t*BuSH) had a series of poorly separated peaks between 191 and 320 cm^{-1}, in addition to a peak at 543 cm^{-1} (Figure 2). The pattern is similar to that reported previously for 2H-NbS_2.[21] The Raman pattern obtained for the TaS_2 films had a large peak between 233 and 301 cm^{-1} and a second broad peak at 365 cm^{-1}. This Raman pattern does not correspond with any reported for TaS_2. However, the Raman pattern is similar to that obtained for 3R-NbS_2, suggesting that the 3R-TaS_2 polytype has been formed. Furthermore, Raman spectroscopy of the niobium and tantalum disulfide films indicated the absence of graphitic carbon in the films despite the use of a carbon-containing solvent being used to create the aerosol.

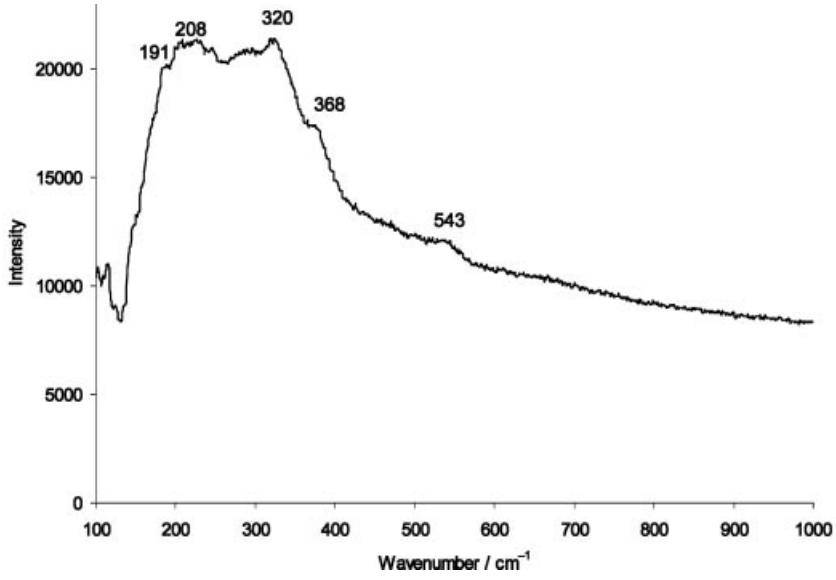

Figure 2. Raman pattern obtained for the film formed on glass from the AACVD reaction of $[Nb(NMe_2)_5]$ and *t*BuSH in dichloromethane at 300 °C.

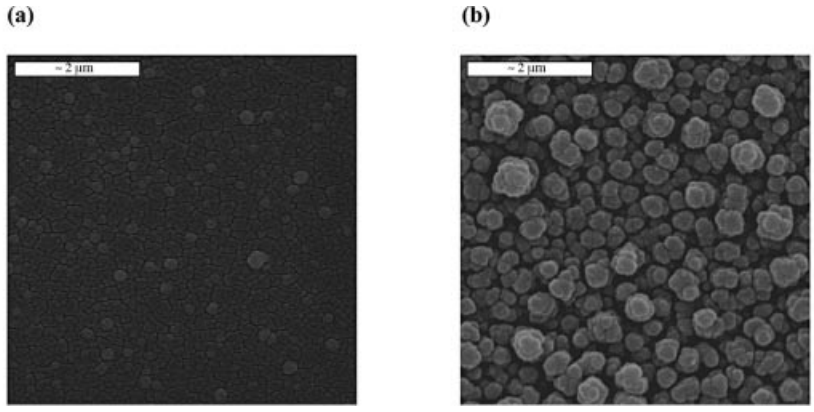

Figure 3. SEM images for films deposited by AACVD from the in situ reaction of $[Nb(NMe_2)_5]$ and *t*BuSH (**a**) in hexanes at 250 °C and (**b**) in dichloromethane at 350 °C.

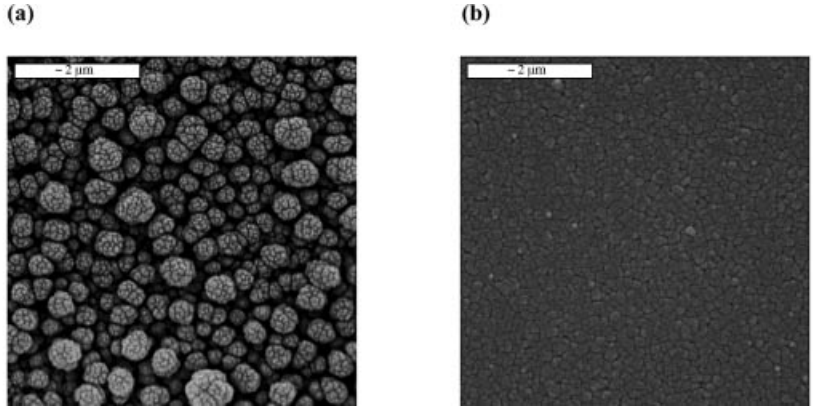

Figure 4. SEM images for films deposited by AACVD at 350 °C from the in situ reaction of $[Ta(NMe_2)_5]$ and *t*BuSH in (**a**) hexanes and (**b**) dichloromethane.

The film morphology was studied using SEM, which showed that the NbS_2 and TaS_2 films grew by an island growth-type mechanism. Individual clusters are clearly visible in the NbS_2 images with cluster size of 0.6 μm and 0.4 μm for films deposited from dichloromethane and hexanes, respectively (Figure 3). The NbS_2 films deposited from hexanes were more uniform than when dichloromethane was used as the solvent. However, the reverse was observed for TaS_2, with films deposited from dichloromethane being more uniform with clusters of 0.4 μm in diameter in comparison with those using hexanes, which had a diameter of 0.8 μm (Figure 4).

The successful formation of NbS_2 and TaS_2 thin films from the in situ AACVD reaction of $[M(NMe_2)_5]$ and *t*BuSH indicates that there is no need to prepare, isolate and purify a metal thiolate single-source precursor, such as $[M(S\text{-}tBu)_5]$. The use of excess *t*BuSH in the AACVD reactions resulted in little oxygen contamination and pre-treating the coater led to more adherent and uniform films. The mechanism for the deposition process was not investigated. However, the decomposition of $[Ti(S\text{-}tBu)_4]$ to TiS_2 has been described previously, and it is likely that the formation of MS_2 (M = Nb, Ta) films described herein would follow a similar mechanism.[22] Thus, the byproducts formed during the deposition of TiS_2 from $[Ti(S\text{-}tBu)_4]$ were principally isobutylene and *tert*-butyl thioalcohol, along with smaller amounts of isobutene, di-*tert*-butyl disulfide, H_2S and di-*tert*-butyl sulfide. The formation of these byproducts was thought to be the result of both β-hydrogen abstraction and a proton-transfer mechanism.[22] In the absence of a sulfur precursor, $[M(NMe_2)_5]$ produces amorphous metal carbonitride coatings.[23] Therefore, the decomposition of $[M(NMe_2)_5]$ can be considered to be the baseline in terms of the coating produced. The reaction of *t*BuSH with $[M(NMe_2)_5]$ results in facile elimination of Me_2NH either via gas phase or surface reactions, due to the presence of the acidic hydrogen in *tert*-butyl thiol. Notably the coatings produced from these reactions contained minimal nitrogen incorporation and even at low substrate temperatures formed MS_2 films with no MN_xC_y incorporation. We attribute this to the fact that the decomposition of $[M(NMe_2)_5]$ is slower than its reaction with *tert*-butyl thiol.

Synthesis

In order to gain an insight into compounds present in the aerosol mist of the AACVD reactions described above, the reaction of $[Ta(NMe_2)_5]$ with five equivalents of *t*BuSH was carried out in toluene at room temperature. An immediate color change from pale yellow to bright orange occurred. After work-up a dark orange oil resulted, which

produced large yellow crystals, on cooling a concentrated dichloromethane solution to –20 °C, in a 47% yield. $^1H/^{13}C$ NMR spectroscopic data obtained from solutions of these crystals were consistent with the formation of the neutral species $[Ta(S\text{-}tBu)_2(NMe_2)_3]$ (Scheme 1). The structure of $[Ta(S\text{-}tBu)_2(NMe_2)_3]$ was confirmed by X-ray crystallography, the results of which are shown in Figure 5. Selected bond lengths and angles are detailed in Table 2. The structure of $[Ta(S\text{-}tBu)_2(NMe_2)_3]$ is monoclinic and crystallizes in the *C*2/*c* space group with the metal on a twofold axis. The tantalum centre in $[Ta(S\text{-}tBu)_2(NMe_2)_3]$ adopts a distorted trigonal bipyramidal geometry with a S–Ta–S bond angle of 166°. Therefore, the two thiolate ligands take up axial positions, with the equatorial sites occupied by the three NMe_2 groups. The Ta–S bonds are 2.47 Å in length and are comparable to those in the reported tantalum thiolate $[Ta(S\text{–}2,6\text{-}Me_2C_6H_3)_4(NMe_2)]$ (2.39–2.43 Å).[17] Ta–N bonds lengths are in the range 1.94–1.97 Å and again compare well with those in $[Ta(S\text{-}2,6\text{-}Me_2C_6H_3)_4(NMe_2)]$ (1.92 Å). The formation of $[Ta(S\text{-}tBu)_2(NMe_2)_3]$ suggests that in the AACVD reaction a mixture of $[M(S\text{-}tBu)_x(NMe_2)_{5-x}]$ (x = 0–5) may be present. However, it is worth noting that a larger excess of thiol is present in the AACVD reaction and so the formation of the homoleptic metal thiolate is possible.

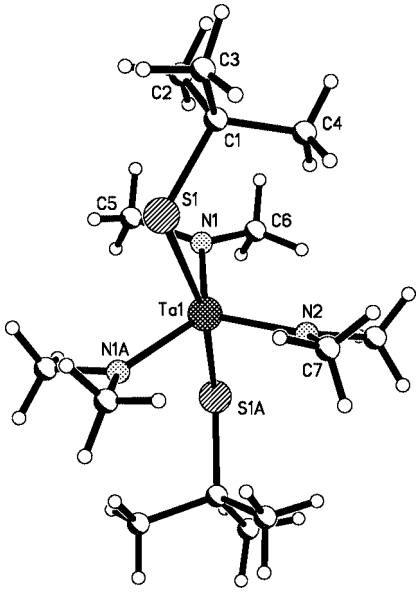

Figure 5. The molecular structure of $[Ta(S\text{-}tBu)_2(NMe_2)_3]$.

Table 2. Selected bond lengths [Å] and angles [°] for $[Ta(S\text{-}tBu)_2(NMe_2)_3]$.

Ta(1)–N(2)	1.939(9)	Ta(1)–S(1)	2.4698(19)
Ta(1)–N(1)	1.968(7)		
N(2)–Ta(1)–N(1)	116.0(2)	N(1A)–Ta(1)–N(1)	128.1(4)
N(2)–Ta(1)–S(1)	96.88(5)	N(1A)–Ta(1)–S(1)	80.4(2)
N(1)–Ta(1)–S(1)	93.5(2)	S(1)–Ta(1)–S(1A)	166.24(10)

Further evidence for the formation of a mixture of complexes in the AACVD reaction was obtained from the reaction of $[Nb(NMe_2)_5]$ with five equivalents of *t*BuSH in toluene at room temperature. After work-up a red/brown oil resulted which was shown by ^1H and ^{13}C NMR to consist of a mixture of products. Thus, in the ^1H NMR of the red/brown oil a number of peaks were observed for each proton environment (*t*Bu, NMe_2) suggesting the formation of a mixture of products of the type $[Nb(S\text{-}tBu)_x(NMe_2)_{5-x}]$ (x = 0–5). The formation of $[Nb(S\text{-}tBu)_x(NMe_2)_{5-x}]$ is in agreement with previous reports of the reaction which suggest that complete substitution of the metal amide ligands by thiolate groups is not achieved.[16,17] Attempts to purify the red/brown oil by recrystallization and distillation were unsuccessful.

Conclusions

Thin films of NbS_2 and TaS_2 can be grown from $[M(NMe_2)_5]$ and *t*BuSH under AACVD conditions. This represents the first deposition of TaS_2 by CVD and the first AACVD formation of NbS_2 and TaS_2 films. Furthermore, the in situ reaction of $[M(NMe_2)_5]$ and *t*BuSH eliminates the need for the synthesis, isolation and purification of a single-source metal thiolate precursor. The solution phase reaction of $[Ta(NMe_2)_5]$ and *t*BuSH resulted in the isolation of $[Ta(S\text{-}tBu)_2(NMe_2)_3]$, which has been structurally characterized. The formation of $[Ta(S\text{-}tBu)_2(NMe_2)_3]$ suggests that a mixture of species of the type $[M(S\text{-}tBu)_x(NMe_2)_{5-x}]$ may be present in the aerosol bubbler. However, due to the large excess of thiol present in the AACVD reactor, it is possible that the homoleptic metal thiolate forms in solution.

Experimental Section

Depositions were carried out under dinitrogen (99.99% from BOC). Precursors were placed in a round-bottomed glass bubbler and a mist was created using a PIFCO HEALTH ultrasonic humidifier (product no. 1077). The solvent mist was transported in a flow of cold nitrogen from the bubbler in an 8-mm gauge pipe to a mixing chamber and then to a horizontal bed, cold-wall reactor with a carbon-heating block containing two Whatman cartridge heaters. Aerosol droplet sizes were calculated to be 50–60 μm.[18] A top plate was suspended 0.5 cm above the glass substrate to ensure a laminar flow. Films were deposited on pieces of 150 mm × 47 mm × 4 mm SiCO-coated float glass (SiCO is a coating containing Si, O and C. It is an effective blocking layer that prevents diffusion of ions in the glass into the coating). The transition metal thiolate complex was generated in situ from the reaction of $[M(NMe_2)_5]$ with excess *t*BuSH (0.3 g $[M(NMe_2)_5]$, M = Ta (0.74 mmol), Nb (0.96 mmol), *t*BuSH 1.0 mL, 8.87 mmol) in solvent (80 mL). Pentakis(dimethylamido)tantalum $[Ta(NMe_2)_5]$ was supplied by Epichem Ltd. and used without further purification, $[Nb(NMe_2)_5]$ was prepared using literature procedures.[16] *t*BuSH was purchased from Aldrich, dried with molecular sieves and degassed. Excess thiol was used in order to minimize the risk of producing partially oxidized films. The reagents were left to react for 1 h prior to the start of each deposition. The *t*BuSH was placed in solvent (60 mL) and the coater was pre-treated with the thiol (1.0 mL) for 20 minutes prior to deposition. Depositions were carried out in either dichloromethane or hexanes at a flow rate of 1.0 $Lmin^{-1}$ over a range of substrate temperatures (225–450 °C).

Dichloromethane was distilled from CaH_2 prior to use; hexanes and toluene were dried using sodium/benzophenone. The experiment was contained in a fume cupboard and the exhaust gases passed through three bleach bubblers. At the end of the deposition the bubbler line was closed and nitrogen was passed over the substrate. The glass substrate was cooled to ca. 60 °C before it was removed. The substrates were cut into ca. 4 cm × 1 cm strips for analysis by SEM, XPS, Raman and UV studies. 3 cm × 2 cm strips were used for X-ray diffraction. Film adherence to the glass was assessed using the Scotch tape test and by scratching the surface using brass and steel.

X-ray powder diffraction patterns were measured with a Siemens D5000 diffractometer using monochromated Cu-$K_{\alpha1}$ radiation (λ_1 = 1.5406 Å). The diffractometer used glancing incident radiation (1.5°). EDXA was obtained with a JOEL 35CF and SEM was obtained with a Hitachi S570 instrument using the KEVEX system. X-ray photoelectron spectra were recorded using a VG ESCALAB 220i XL instrument using focused (300 μm spot) monochromatic Al-K_α radiation at a pass energy of 20 eV. Scans were acquired with steps of 50 meV. A flood gun was used to control charging and the binding energies were referenced to an adventitious C 1s peak at 284.8 eV. Depth profile measurements were obtained by using argon beam sputtering. Reflectance and transmission spectra were recorded between 300 and 1200 nm by a Zeiss minature spectrometer. Reflectance measurements were standardized relative to a rhodium mirror and transmission relative to air. Raman spectra were acquired with a Renishaw Raman System 1000 using a helium-neon laser of wavelength 632.8 nm. The Raman system was calibrated against the emission lines of neon. NMR spectra were recorded with a Bruker AMX400 spectrometer at UCL, referenced to CD_2Cl_2, which was dried and degassed over molecular sieves prior to use. ^1H and ^{13}C chemical shifts are reported relative to $SiMe_4$ (δ, 0.00). Single-crystal X-ray data were collected with a Bruker SMART APEX CCD diffractometer.

AACVD Reaction of [Nb(NMe$_2$)$_5$] and *t*BuSH: *t*BuSH (1.0 mL, 8.87 mmol) was placed in 60 mL of solvent in the AACVD bubbler and used to pre-treat the reactor for 5 min before the addition of the niobium precursor. After pre-treating the reactor, [Nb(NMe$_2$)$_5$] (0.3 g, 0.96 mmol) in 15 mL of solvent was added to the bubbler. An orange solution formed immediately, and the mixture was reacted for 60 minutes before each deposition was started.

AACVD reaction of [Ta(NMe$_2$)$_5$] and *t*BuSH: The experimental procedure was the same as for the AACVD reaction of [Nb(NMe$_2$)$_5$] and *t*BuSH but [Ta(NMe$_2$)$_5$] (0.3 g, 0.74 mmol) was used in place of [Nb(NMe$_2$)$_5$].

Reaction of [Nb(NMe$_2$)$_5$] and *t*BuSH: 2-Methylpropanethiol (0.4 mL, 1.60 mmol) was added to a stirred solution of [Nb(NMe$_2$)$_5$] (0.2 g, 0.64 mmol) in toluene (30 mL). An immediate color change from pale orange to deep red occurred on addition of the thiol. Stirring was continued for 4 h and the solution was concentrated in vacuo to give a dark red/brown oil. ^1H NMR (CD_2Cl_2): δ = 1.2 [s, (CH_3)$_3$CS], 1.3 [s, (CH_3)$_3$CS], 1.4 [s, (CH_3)$_3$CS], 1.6 [s, (CH$_3$)$_3$CS*H*], 3.45 (s, N*Me*$_2$), 3.55 (s, N*Me*$_2$) ppm. $^{13}C\{^1H\}$ NMR (CD_2Cl_2): δ = 30.7 [(*C*H$_3$)$_3$CS], 31.7 [(*C*H$_3$)$_3$CS], 34.6 [(CH$_3$)$_3$CSH], 35.0 [(CH$_3$)$_3$*C*S], 35.7 [(*C*H$_3$)$_3$CS], 49.0 (s, N*Me*$_2$), 50.6 (s, N*Me*$_2$) ppm.

Synthesis of [Ta(S-*t*Bu)$_2$(NMe$_2$)$_3$]: 2-Methylpropanethiol (0.14 mL, 1.25 mmol) was added to a stirred solution of [Ta(NMe$_2$)$_5$] (0.1 g, 0.25 mmol) in toluene (20 mL). Stirring was continued for 16 h resulting in a dark orange solution. The solvent was removed in vacuo to give an orange-brown oil. This oil was redissolved in ca. 2 mL of hexanes and cooled to –20 °C. Large, rectangular, pale yellow crystals (0.06 g, 47%) suitable for X-ray analysis were formed. ^1H NMR (CD_2Cl_2): δ = 1.25 [s, 18 H, (CH_3)$_3$CS], 3.45 (s, 18 H, N*Me*$_2$) ppm. $^{13}C\{^1H\}$ NMR (CD_2Cl_2): δ = 36.0 [(*C*H$_3$)$_3$CS], 42.0 [(CH$_3$)$_3$*C*S], 47.3 (N*Me*$_2$) ppm. $C_{14}H_{36}N_3TaS_2$ (491): calcd. C 34.2, H 7.38, N 8.55; found C 34.1, H 7.5, N 8.1. M.p. 105 °C.

Caution: It should be noted that the AACVD reaction of [M(NMe$_2$)$_2$] (M = Nb, Ta) and *t*BuSH could conceivably produce H_2S. Care should be taken to conduct all experiments in a fume cupboard.

X-ray Crystallography: Crystals of [Ta(S-*t*Bu)$_2$(NMe$_2$)$_3$] were grown from hexanes at –20 °C. Yellow rectangular crystals 0.50 × 0.50 × 0.10 mm, M_r = 491.53, monoclinic, *C*2/*c*, *a* = 10.2460(14), *b* = 15.052(2), *c* = 13.2966(18) Å, β = 92.855(2)°, *V* = 2048.1(5) Å^3, ρ(calcd.) = 1.594 g cm^{-3}, *Z* = 4, Mo-K_α (λ = 0.71073 Å), 150 K, 7531 reflections measured, 2376 independent, μ(Mo-K_α) = 5.567 mm^{-1}, T_{max} –0.600, T_{min} = 0.1673, structure solved by direct methods (SHELXS) and refined on F^2 (SHELXL97), 98 parameters, all non-hydrogen atoms anisotropic, hydrogen atoms refined with riding model, R = 0.0578, wR_2 = 0.1376 (all data), R = 0.0551, wR_2 = 0.1353 [$I > 2\sigma(I)$], largest residual 3.6 e Å^3, close to the metal atom.

CCDC-256491 contains the supplementary crystallographic data for this paper. These data can be obtained free of charge from The Cambridge Crystallographic Data Centre via www.ccdc.cam.ac.uk/data_request/cif.

Acknowledgments

I. P. P. thanks the EPSRC for grant GR/M82592 for purchase of the Renishaw Raman microscope. E. S. P. thanks the EPSRC for a studentship. Epichem Ltd. is thanked for supplying [Ta(NMe$_2$)$_5$].

[1] S. Whittingham, *Prog. Solid State Chem.* **1978**, *12*, 41.
[2] K. Ellmer, C. Stock, K. Diesner, I. Sieber, *J. Cryst. Growth* **1997**, *182*, 389.
[3] M. Regula, C. Ballif, J. H. Moser, F. Levy, *Thin Solid Films* **1995**, *289*, 67.
[4] L. Hernan, J. Morales, L. Sánchez, J. L. Tirado, *Electrochim. Acta* **1994**, *39*, 2665.
[5] W. M. R. Divigalpitiya, R. F. Frindt, S. R. Morrison, *J. Phys. D: Appl. Phys.* **1990**, *23*, 966.
[6] C. Geantet, J. Afonso, M. Breyesse, N. Allali, M. Danot, *Catal. Today* **1996**, *28*, 23.
[7] V. Gaborit, N. Allali, C. Geantet, M. Breysse, M. Vrinat, M. Danot, *Catal. Today* **2000**, *57*, 267.
[8] P. Afanasiev, L. Fischer, F. Beauchesne, M. Danot, V. Gaborit, M. Breysse, *Catal. Lett.* **2000**, *64*, 59.
[9] N. Allali, E. Prouzet, A. Michalowicz, V. Gaborit, A. Nadiri, M. Danot, *Appl. Catal. A* **1997**, *159*, 333.
[10] W. M. R. Divigalpitya, R. F. Frindt, S. R. Morrison, *Science* **1989**, *246*, 369.
[11] P. J. McKarns, M. J. Heeg, C. H. Winter, *Inorg. Chem.* **1998**, *37*, 4743.
[12] C. J. Carmalt, C. W. Dinnage, I. P. Parkin, A. J. P. White, D. J. Williams, *Inorg. Chem.* **2002**, *41*, 3668.
[13] C. J. Carmalt, T. D. Manning, I. P. Parkin, E. S. Peters, A. L. Hector, *J. Mater. Chem.* **2004**, *14*, 290.
[14] T. Shimada, F. S. Ohuchi, A. Koma, *Surf. Sci.* **1993**, *291*, 57.
[15] H. Enomoto, T. Kawano, M. Kawaguchi, Y. Takano, K. Sekizawa, *Jpn. J. Appl. Phys. Lett.* **2004**, *43*, L123.
[16] D. C. Bradley, P. A. Hammersley, *J. Chem. Soc. (A)* **1967**, 1894.
[17] C. J. Carmalt, C. W. Dinnage, I. P. Parkin, A. J. P. White, D. J. Williams, *J. Chem. Soc. Dalton Trans.* **2001**, 2554.

[18] R. J. Lang, *J. Acoustical Soc. Am.* **1962**, *34*, 6.
[19] G. E. McGuire, G. K. Schweitzer, T. A. Carlson, *Inorg. Chem.* **1973**, *12*, 2451.
[20] K. Dartigeas, L. Benoist, D. Gonbeau, G. Pfister-Guillouzo, G. Ouvrard, A. Levasseur, *J. Electron Spectrosc. Relat. Phenom.* **1997**, *83*, 45.
[21] W. G. McMullan, J. C. Irwin, *Solid State Commun.* **1983**, *45*, 557.
[22] J. Cheon, J. E. Gozum, G. S. Girolami, *Chem. Mater.* **1997**, *9*, 1847.
[23] R. Fix, R. Gordon, D. M. Hoffman, *Chem. Mater.* **1990**, *2*, 235.

Received: May 4, 2005
Published Online: September 9, 2005

